

Structural Constraints from Proton-Mediated Rare-Spin Correlation Spectroscopy in Rotating Solids[†]

Adam Lange, Sorin Luca, and Marc Baldus*

Max-Planck-Institute for Biophysical Chemistry, Solid-State NMR, Department for NMR-based Structural Biology, Am Fassberg 11, 37077 Göttingen, Germany

Received April 26, 2002

Much of the success of solution-state nuclear magnetic resonance (NMR) in determining three-dimensional (3D) structures relates to the high abundance of short proton–proton distances that can characterize the 3D fold of a biomolecule.¹ Combined with ¹H evolution and detection periods, NOESY²-related correlation experiments today represent standard methods to detect (¹H,¹H) contacts in high sensitivity and resolution. Proton correlation experiments have also been suggested for use in the solid-state,³ but the size of dipolar proton–proton interactions and the limited spectral dispersion among ¹H resonances under magic angle spinning (MAS⁴) conditions have thus far made biophysical applications challenging.

We here demonstrate that a variety of nontrivial proton–proton contacts can be observed in the solid-state when encoded in high-resolution rare-spin evolution and detection periods. For this purpose, radio frequency (rf) schemes should allow for a rapid through-space (¹H,¹H) polarization transfer and minimize relaxation losses. We have investigated the spin-locking and nutation behavior of ¹H NMR signals in a protonated peptide as a function of the applied rf amplitude ω_1 and MAS rate ω_R . In contrast to rare-spin correlation spectroscopy,⁵ one experimentally finds that the ¹H relaxation behavior is strongly dependent on the ratio $\kappa = \omega_1/\omega_R$ and generally favors very small or large values of κ (see Supporting Information). NHHC and CHHC correlation schemes that encode (¹H,¹H) contacts in high resolution and are compatible with these experimental requirements are depicted in Figure 1. For sensitivity reasons, the final cross polarization (CP) transfer step and the detection periods involve ¹³C nuclei. (¹H,¹H) contact is established using zero-quantum (0Q) longitudinal mixing (a) or POST-C7⁶ double-quantum (2Q) polarization transfer (b). In both cases, the (¹H,¹H) transfer step is enclosed by a set of two short (t_{NH} , t_{CH}) heteronuclear CP segments that ensure polarization transfer within NH or CH_x groups only. An additional z-filter time t_D (3 ms) prior to the t_1 evolution maximizes the efficiency of the $t_{(C,N)H}$ CP transfer by dephasing transversal proton magnetization. 0Q-CHHC type experiments have previously been suggested for the detection of weak dipolar interactions and were analyzed within a classical spin diffusion approximation.⁷ Similar to the NOE analysis of solution-state biomolecules, probing the strongest dipolar (¹H,¹H) interactions in biomolecules is of interest to us herein.

In Figure 2 (a) and (b) we present 0Q-NHHC and 0Q-CHHC correlation experiments on a uniformly [¹³C,¹⁵N]-labeled version of the tripeptide AGG at 11 kHz MAS. In contrast to conventional rare-spin spectra^{5,8} a variety of interesting correlations are detected. For the selected mixing times, C $\alpha(i)$ –NH($i+1$) and C $\alpha(i)$ –C $\alpha(i+1)$ correlations are observed that corroborate the sequential assignments

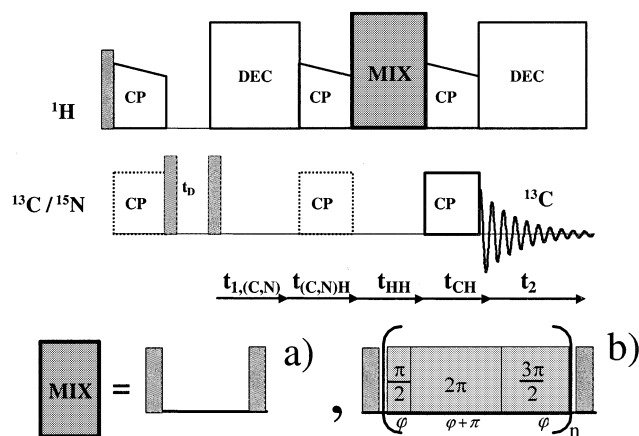


Figure 1. Experimental NHHC and CHHC correlation schemes with (a) longitudinal and (b) double-quantum POST-C7⁶ mixing. For NHHC experiments, evolution and the first two CP rare-spin pulses are performed on the ¹⁵N channel. The CHHC method and the final CP transfer step of the NHHC experiment involve ¹³C spectroscopy. Unless stated otherwise, shaded pulses correspond to 90° nutations. All experiments were conducted at 11 kHz MAS leading to ¹H rf amplitudes of 77 kHz during 2Q mixing. Further details regarding the pulse scheme are given in the Supporting Information.

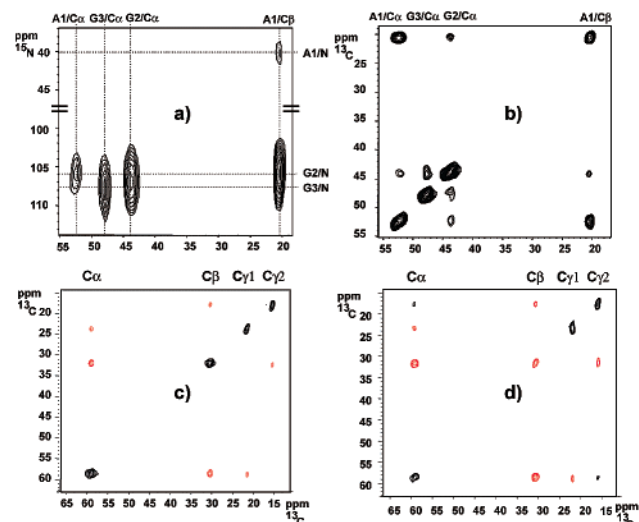


Figure 2. Experimental NHHC (a) and CHHC (b) 0Q-correlation spectra on U-[¹³C,¹⁵N] AGG (indicated numbering starts at N terminus) for homonuclear contact times t_{HH} of 500 and 200 μ s, respectively. In (c) and (d) results of a 2Q-CHHC experiments on FMOCC U-[¹³C,¹⁵N] valine for mixing times of 208 μ s (c) and 312 μ s (d) are shown. Negative cross-peak intensities are indicated in red.

previously obtained from NCOCA and NCACB correlation experiments.⁹ In Figure 2b the strongest cross-peaks are detected for the

* To whom correspondence should be addressed. Telephone: (+49)-551-2012212. Fax: (+49)-551-2012202. E-mail: maba@nmr.mpiibpc.mpg.de.
[†] Presented in part at the 43rd ENC meeting, Asilomar, CA, April 14–19, 2002.

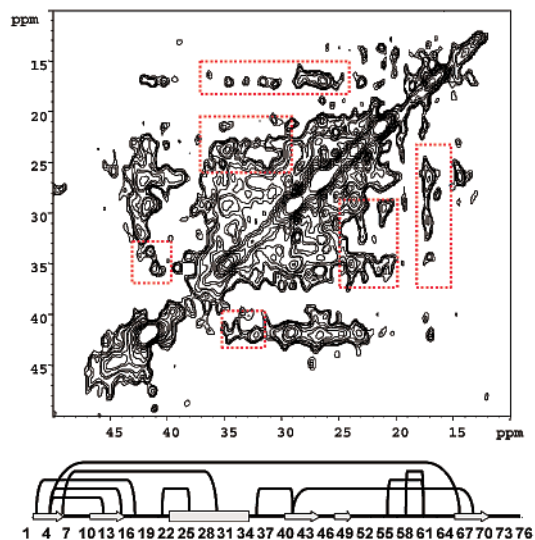


Figure 3. Experimental CHHC 0Q-correlation data ($t_{HH} = 500 \mu\text{s}$) obtained on a uniformly labeled version of ubiquitin (5 mg, VLI Research, Malvern, PA). Only the side-chain region [50 ppm, 10 ppm] is shown. The data set was recorded on a 600 MHz instrument for 2.5 days. Interresidue contacts that result from correlations well-resolved in the spectrum are indicated along the polypeptide chain. See also Supporting Information.

shortest (intraresidue) $H_{\alpha}-H_{\beta}$ distance, indicating that the selected mixing times here encode qualitative information about intramolecular ($^1\text{H}, ^1\text{H}$) distances. Data obtained at 400 and 600 MHz (^1H resonance frequency) moreover show that the shortest distances dominate the correlation patterns for ($^1\text{H}, ^1\text{H}$) mixing times up to about $500 \mu\text{s}$. In addition, the 2Q transfer mechanism of Figure 2c,d offers the possibility to distinguish between direct and relay ($^1\text{H}, ^1\text{H}$) mixing. For example, Figure 2c contains 2Q-CHHC results on Fmoc U- $^{13}\text{C}, ^{15}\text{N}$ -labeled valine for a homonuclear mixing time of $208 \mu\text{s}$. Here, nearest-neighbor interactions are characterized by negative cross-peak intensities consistent with 2Q polarization transfer within a proton pair.¹⁰ For longer mixing times, positive cross-peak intensities due to relay transfer involving an odd (three or higher) number of ^1H spins are observed.¹¹ Again, the cross-peak pattern is dominated by nearest-neighbor ($^1\text{H}, ^1\text{H}$) interactions, and the spectra reveal direct information about the 3D arrangement of Fmoc-Val. For example, one observes only one set of C_{α} -methyl and C_{β} -methyl correlations indicative for a Fmoc-induced break of molecular symmetry in comparison to the highly symmetric arrangement of valine (data not shown).

Since the underlying NHHC and CHHC polarization transfer involves through-space ($^1\text{H}, ^1\text{H}$) contacts, we finally investigate whether the presented approach also allows for the detection of medium-to-long-range structural constraints¹ in larger systems. For example, Figure 3 contains the CHHC correlation pattern of a U- $^{13}\text{C}, ^{15}\text{N}$ -labeled version of ubiquitin revealing a large number of ($^1\text{H}, ^1\text{H}$) contacts. Although the spectral resolution is insufficient to resolve all correlations in the spectrum, a significant fraction of the observed cross-peak intensities can be identified that are *not* observed in a corresponding CC correlation experiment. A subset of these correlations is indicated in the spectrum of Figure 3 (red boxes). Since the X-ray (PDB code: 1UBQ) and solution-state NMR (PDB entry: 1D3Z) derived structures of ubiquitin are largely consistent, we have examined the CHHC spectrum of Figure 3 using resonance assignments obtained in the solid and solution state. On the basis of the experimental results in Figure 2, only ($^1\text{H}, ^1\text{H}$) distance constraints (derived from 1D3Z) of 2.5 \AA or shorter were considered for the spectral analysis. Well-resolved cross-peak intensities reflecting medium-to-long-range contacts are summarized

in Figure 3 (see Supporting Information) and indicate interresidue contacts throughout the polypeptide chain. Similar to the solution state¹, a further structural analysis could involve the study of the experimentally observed cross-peak buildup rates, possibly in conjunction with a set of 2Q correlation data that separate direct and relay transfer. For applications at 11 kHz MAS we found the 0Q schemes to be superior (25% efficiency of direct CP signal) in comparison to the suggested 2Q methods. In the latter case, the utilization of higher MAS rates or the development of tailored rf schemes that maximize the transfer efficiency could be beneficial.

In summary, we have introduced a general concept to probe through-space ($^1\text{H}, ^1\text{H}$) contacts of protonated solid-phase systems in high spectral resolution. In the current context, the observed correlations were used to infer sequential assignments in a tripeptide and for a qualitative structural analysis of solid-phase biomolecules. In contrast to (C,C) or (N,C) correlation methods where the strongest dipolar interactions are of limited structural information,^{8,12} nearest-neighbor ($^1\text{H}, ^1\text{H}$) correlations not only reflect backbone or side chain conformation in polypeptides, but they can also characterize the 3D fold of the molecule of interest. The presented approach hence allows for the study of the complete molecular arrangement of a uniformly labeled molecule without advanced isotope-labeling methods¹³ or chemical shift selective rf pulse schemes.¹⁴ We expect the concept to be of general use for a variety of systems ranging from applications in inorganic chemistry to biophysical studies in fibrous and membrane proteins.

Acknowledgment. We thank H. Förster (Bruker/Germany) for technical support and B. Angerstein for help during the preparation of the manuscript.

Supporting Information Available: Further details of the pulse scheme, (C,C) correlation data on ubiquitin and the resonance assignments utilized in Figure 3 (PDF). This material is available free of charge via the Internet at <http://pubs.acs.org>.

References

- Wüthrich, K. *NMR of Proteins and Nucleic Acids*; Wiley-Interscience: New York, 1986.
- Jeener, J.; Meier, B. H.; Bachmann, P.; Ernst, R. R. *J. Chem. Phys.* **1979**, *71*, 4546–4553.
- Sakellariou, D.; Lesage, A.; Emsley, L. *J. Am. Chem. Soc.* **2001**, *123*, 5604–5605. Brown, S. P.; Spiess, H. W. *Chem. Rev.* **2001**, *101*, 4125–4155.
- Andrew, E. R.; Bradbury, A.; Eades, R. G. *Nature* **1958**, *182*, 1659.
- Griffin, R. G. *Nat. Struct. Biol.* **1998**, *5*, 508–512.
- Hohwy, M.; Jakobsen, H. J.; Eden, M.; Levitt, M. H.; Nielsen, N. C. *J. Chem. Phys.* **1998**, *108*, 2686–2694.
- Wilhelm, M.; Feng, H.; Tracht, U.; Spiess, H. W. *J. Magn. Reson.* **1998**, *134*, 255–260. Mulder, F. M.; Heinen, W.; van Duin, M.; Lugtenburg, J.; de Groot, H. J. M. *J. Am. Chem. Soc.* **1998**, *120*, 12891–12894. Wei, Y. F.; Ramamoorthy, A. *Chem. Phys. Lett.* **2001**, *342*, 312–316.
- Baldus, M. *Prog. Nucl. Magn. Reson. Spectrosc.* **2002**, In press.
- Luca, S.; Filippov, D. V.; van Boom, J. H.; Oschkinat, H.; de Groot, H. J. M.; Baldus, M. *J. Biomol. NMR* **2001**, *20*, 325–331.
- Baldus, M.; Tomaselli, M.; Meier, B. H.; Ernst, R. R. *Chem. Phys. Lett.* **1994**, *230*, 329–336.
- Sun, B. Q.; Costa, P. R.; Kocisko, D.; Lansbury, P. T.; Griffin, R. G. *J. Chem. Phys.* **1995**, *102*, 702–707.
- Kiihne, S.; Mehta, M. A.; Stringer, J. A.; Gregory, D. M.; Shiels, J. C.; Drobny, G. P. *J. Phys. Chem. A* **1998**, *102*, 2274–2282. Hohwy, M.; Rienstra, C. M.; Jaroniec, C. P.; Griffin, R. G. *J. Chem. Phys.* **1999**, *110*, 7983–7992. Brinkmann, A.; Eden, M.; Levitt, M. H. *J. Chem. Phys.* **2000**, *112*, 8539–8554. Ladizhansky, V.; Vega, S. *J. Chem. Phys.* **2000**, *112*, 7158–7168.
- LeMaster, D. M.; Kushlan, D. M. *J. Am. Chem. Soc.* **1996**, *118*, 9255–9264. Gardner, K. H.; Kay, L. E. *Annu. Rev. Biophys. Biomol. Struct.* **1998**, *27*, 357–406. Hong, M.; Jakes, K. *J. Biomol. NMR* **1999**, *14*, 71–74.
- Takegoshi, K.; Nomura, K.; Terao, T. *J. Magn. Reson.* **1997**, *127*, 206–216. Baldus, M.; Petkova, A. T.; Herzfeld, J.; Griffin, R. G. *Mol. Phys.* **1998**, *95*, 1197–1207. Jaroniec, C. P.; Toungue, B. A.; Herzfeld, J.; Griffin, R. G. *J. Am. Chem. Soc.* **2001**, *123*, 3507–3519.

JA026691B